Since January 2020 Elsevier has created a COVID-19 resource centre with free information in English and Mandarin on the novel coronavirus COVID-19. The COVID-19 resource centre is hosted on Elsevier Connect, the company's public news and information website.

ORIGINAL ARTICLE

Lung Cancer Models Reveal Severe Acute Respiratory Syndrome Coronavirus 2–Induced Epithelial-to-Mesenchymal Transition Contributes to Coronavirus Disease 2019 Pathophysiology

C. Allison Stewart, PhD,[a] Carl M. Gay, MD, PhD,[a] Kavya Ramkumar, PhD,[a] Kasey R. Cargill, PhD,[a] Robert J. Cardnell, PhD,[a] Monique B. Nilsson, PhD,[a] Simon Heeke, PhD,[a] Elizabeth M. Park, PhD,[a] Samrat T. Kundu, PhD,[a] Lixia Diao, PhD,[b] Qi Wang, PhD,[b] Li Shen, MS,[b] Yuanxin Xi, PhD,[b] Bingnan Zhang, MD,[a] Carminia Maria Della Corte, MD,[c] Youhong Fan, BS,[a] Kiran Kundu, PhD,[a] Boning Gao, PhD,[d] Kimberley Avila, BS,[d] Curtis R. Pickering, PhD,[e] Faye M. Johnson, MD, PhD,[a] Jianjun Zhang, MD, PhD,[a] Humam Kadara, PhD,[f] John D. Minna, MD,[d] Don L. Gibbons, MD, PhD,[a] Jing Wang, PhD,[b] John V. Heymach, MD, PhD,[a] Lauren Averett Byers, MD, MS[a,*]

[a]*Department of Thoracic/Head & Neck Medical Oncology, The University of Texas MD Anderson Cancer Center, Houston, Texas*
[b]*Department of Bioinformatics and Computational Biology, The University of Texas MD Anderson Cancer Center, Houston, Texas*
[c]*Oncology Division, Department of Precision Medicine, University of Campania "Luigi Vanvitelli," Naples, Italy*
[d]*Department of Internal Medicine and Pharmacology, Hamon Center for Therapeutic Oncology Research, The University of Texas Southwestern Medical Center, Dallas, Texas*
[e]*Department of Head and Neck Surgery, The University of Texas MD Anderson Cancer Center, Houston, Texas*
[f]*Department of Translational Molecular Pathology, The University of Texas MD Anderson Cancer Center, Houston, Texas*

Received 4 February 2021; revised 2 June 2021; accepted 2 July 2021
Available online - 16 July 2021

ABSTRACT

Introduction: Coronavirus disease 2019 is an infectious disease caused by severe acute respiratory syndrome coronavirus 2 (SARS-CoV-2), which enters host cells through the cell surface proteins ACE2 and TMPRSS2.

Methods: Using a variety of normal and malignant models and tissues from the aerodigestive and respiratory tracts,

*Corresponding author.

Drs. Stewart and Gay contributed equally to this work.

Disclosure: Dr. Byers reports serving on advisory committees for AstraZeneca, AbbVie, GenMab, BergenBio, Pharma Mar SA, Sierra Oncology, Merck, Bristol-Myers Squibb, Genentech, and Pfizer and receiving research support from AbbVie, AstraZeneca, GenMab, Sierra Oncology, and Tolero Pharmaceuticals. Dr. Heymach reports serving on advisory committees for AstraZeneca, Boehringer Ingelheim, Catalyst, Genentech, GlaxoSmithKline, Guardant Health, Foundation Medicine, Hengrui Therapeutics, Eli Lilly, Novartis, Spectrum, Sanofi, Takeda, Mirati Therapeutics, Bristol-Myers Squibb, BrightPath Biotherapeutics, Janssen Global Services, Nexus Health Systems, EMD Serono, Pneuma Respiratory, Kairos Venture Investments, Roche, and Leads Biolabs; receiving research support from AstraZeneca, Bayer, GlaxoSmithKline, and Spectrum; having patents PCT/US2019/024353-UTFC.P1354AE, 62/793,565/PCT/US2020/013889, 62/967,282, 62/895,322-17/011,519, 62/929,840/PCT/US2020/058548, and 62/967,275/UTSC.P1499US.P1; and receiving royalties and licensing fees from Spectrum. Dr. Gibbons reports serving on scientific advisory committees for AstraZeneca, GlaxoSmithKline, Sanofi, and Janssen and receiving research support from Janssen, Takeda, Ribon Therapeutics, Astellas, and AstraZeneca. Dr. Johnson reports receiving donor research funds. Dr. Gay reports receiving research funding from AstraZeneca. Dr. Minna reports receiving royalties and licensing from distribution of cell lines from the National Institutes of Health and The University of Texas Southwestern. Dr. Nilsson reports receiving royalties and licensing fees from Spectrum. Zhang reports receiving grants from Merck and Johnson and Johnson and personal fees from Bristol-Myers Squibb, AZ, GenePlus, and Innovent outside of the submitted work. Dr. Kadara reports receiving grant from Johnson and Johnson. The remaining authors declare no conflict of interest.

Address for correspondence: Lauren Averett Byers, MD, MS, Thoracic/Head and Neck Medical Oncology, The University of Texas MD Anderson Cancer Center, 1515 Holcombe Boulevard, Unit 1443, Houston, TX 77030. E-mail: lbyers@mdanderson.org or lauren@alumni.princeton.edu.

ISSN: 1556-0864
https://doi.org/10.1016/j.jtho.2021.07.002

we investigated the expression and regulation of *ACE2* and *TMPRSS2*.

Results: We find that *ACE2* expression is restricted to a select population of epithelial cells. Notably, infection with SARS-CoV-2 in cancer cell lines, bronchial organoids, and patient nasal epithelium induces metabolic and transcriptional changes consistent with epithelial-to-mesenchymal transition (EMT), including up-regulation of *ZEB1* and *AXL*, resulting in an increased EMT score. In addition, a transcriptional loss of genes associated with tight junction function occurs with SARS-CoV-2 infection. The SARS-CoV-2 receptor, ACE2, is repressed by EMT through the transforming growth factor-β, ZEB1 overexpression, and onset of EGFR tyrosine kinase inhibitor resistance. This suggests a novel model of SARS-CoV-2 pathogenesis in which infected cells shift toward an increasingly mesenchymal state, associated with a loss of tight junction components with acute respiratory distress syndrome-protective effects. AXL inhibition and ZEB1 reduction, as with bemcentinib, offer a potential strategy to reverse this effect.

Conclusions: These observations highlight the use of aerodigestive and, especially, lung cancer model systems in exploring the pathogenesis of SARS-CoV-2 and other respiratory viruses and offer important insights into the potential mechanisms underlying the morbidity and mortality of coronavirus disease 2019 in healthy patients and patients with cancer alike.

Keywords: SARS-CoV-2; EMT; ACE2; NSCLC; ZEB1; AXL

Introduction

In December 2019, reports of a viral illness with severe respiratory symptoms emerged from Wuhan, People's Republic of China.[1,2] The novel virus was classified as a coronavirus and subsequently named severe acute respiratory syndrome coronavirus 2 (SARS-CoV-2). It exhibited rapid global spread and met the WHO's criteria of a pandemic within 3 months after the first reported diagnosis (https://covid19.who.int/). As of April 2021, more than 148 million individuals have been infected worldwide with more than 3.1 million deaths (covid19.who.int). SARS-CoV-2 infection is the cause of the respiratory illness coronavirus disease 2019 (COVID-19), which presents most frequently with symptoms including cough and dyspnea, accompanied by a moderate-to-high fever.[2,3] The severity of patient symptoms after SARS-CoV-2 infection varies widely from asymptomatic carrier status to critical illness. Given the specific complications associated with the infection, it is not initially surprising that patients with cancer and, specifically, thoracic malignancies, seem to experience poorer clinical outcomes.[4,5] Nevertheless, it is unclear whether these poorer outcomes represent the impact of demographics (e.g., age, smoking status, sex) or cellular and molecular changes associated with the tumor and its microenvironment.

Although there are currently no validated molecular biomarkers for susceptibility to, or severity of, SARS-CoV-2 infection, it has recently been described that, as with SARS-CoV, SARS-CoV-2 cell entry requires interactions with ACE2 and TMPRSS2 on the surface of the host cell.[6] Specifically, ACE2 binds to a subunit of the SARS-CoV-2 spike (S) protein, whereas TMPRSS2 is responsible for S-protein cleavage, or priming, to allow fusion of viral and host cellular membranes.[6] Differences in these receptors have been described in certain populations harboring higher allelic frequency of mutations and coding variants associated with higher *ACE2* expression.[7] Notably, ACE2 has previously been found to exert a protective effect toward the development of acute respiratory distress syndrome (ARDS)—one of the most common and lethal complications of SARS-CoV-2 infection.[8,9] Given the propensity for ARDS in SARS-CoV-2–infected patients, this protective effect initially seems paradoxical, but previous data on SARS-CoV-1 suggest that subsequent to infection, ACE2 expression is down-regulated, thus tipping the balance in favor of acute lung injury.[10]

As the presence of ACE2 or TMPRSS2 may be rate limiting for SARS-CoV-2 infection, we used bulk and single-cell transcriptional data from a combination of normal and malignant tissue samples and models from the aerodigestive and respiratory tracts to explore mechanisms governing the expression of *ACE2* and *TMPRSS2*. These data were assembled from a variety of sources, including current and previous works from our laboratory, department, and data sets generated as part of our longstanding joint The University of Texas Southwestern/MD Anderson Cancer Center National Cancer Institute (NCI) Lung SPORE program, including public data sets derived worldwide[11-34] and represent a novel repurposing of data to understand more of ACE2 expression and consequences of infection. Our bulk data suggest that aerodigestive and lung cancer cell lines have a broad range of *ACE2* and *TMRPSS2* expression and would serve as good models for studying SARS-CoV-2 infection, consistent with the observation that SARS-CoV-2 virus has the ability to infect several lung cancer cell lines (e.g., Calu-3 and A549).[6,35] Furthermore, although the normal aerodigestive and respiratory tracts represent key points of viral entry and infection, limiting an investigation to normal tissue may unnecessarily limit available samples for analysis and, especially, limit the

range of cellular and molecular phenomena represented by those samples.

Meanwhile, single-cell analyses reveal that although *TMPRSS2* is widely expressed in normal respiratory epithelium, *ACE2* expression is limited to a small collection of cells[36] and, therefore, may be a limiting factor for infection or drive dependence on other mechanisms, such as putative AXL-mediated cell entry.[37-41] There have been numerous reports of patients developing loss of chemosensation (taste, smell, etc.) after SARS-CoV-2 infection—an observation that pointed to another small collection of cells.[42,43] Tuft, or brush, cells are rare chemosensory cells present in the aerodigestive and respiratory tracts, among other sites, that mediate taste and smell, along with innate immune response.[44,45] These cells, which are epithelial in nature, strongly express *POU2F3*, a transcription factor that is also highly expressed in certain lung cancers, including a subset of SCLC.[46-49] Our analyses indeed suggest that *ACE2* expression is enriched in tuft cells compared with nontuft cells within the respiratory tract. Nevertheless, this was not absolute and, thus, we considered broader regulatory mechanisms that might govern *ACE2* expression. Previous literature has proposed, inconsistently, both positive and negative associations between *ACE2* expression and epithelial differentiation,[50,51] although tuft cells, in which *ACE2* is enriched in our analysis, are highly epithelial.[45] We evaluated the relationship between *ACE2* and epithelial differentiation in numerous aerodigestive and respiratory datasets and found striking and consistent positive correlations with transcriptional, microRNA (miRNA), and metabolic signifiers of epithelial differentiation in virtually all data sets analyzed.

Finally, we consider the role that regulators of epithelial-to-mesenchymal transition (EMT) may play in modulation of *ACE2* expression. EMT is a well-characterized phenomenon critical to normal developmental processes but co-opted by tumor cells to promote metastasis and resistance to treatments ranging from chemotherapies to radiation.[52] We provide evidence that the miR-200 family, ZEB1 pathway, which is an established regulator of EMT,[53,54] also directly regulates *ACE2* expression, likely through putative ZEB1 repressor sites located in the *ACE2* promoter. Furthermore, we highlight that SARS-CoV-2 infection both in vitro and in patients yields increased expression of EMT-associated genes, including *ZEB1* and *AXL* and metabolic derangements (e.g., a shift away from glutamine and toward glutamate) characteristic of EMT.[55,56] Inhibition of AXL, a mesenchymal receptor tyrosine kinase, with bemcentinib both induces ACE2 and represses ZEB1 and may serve as a therapy to shift SARS-CoV-2–infected cells away from a mesenchymal phenotype (i.e., reverse EMT). In addition, viral infection of epithelial cells, which are glutamine dependent with high *GLUL* expression and presumably more metabolically primed for replication, promotes rapid replication owing to the enhanced dependence on glutamine for nucleotide synthesis and subsequently depletes glutamine stores.[56] Other viruses have been found to induce host cell metabolic reprogramming to satisfy the biosynthetic and energy requirements needed for replication.[57-60]

The association between EMT and lung injury or ARDS has been described previously, with the central pathogenesis being the breakdown of the alveolar-epithelial barrier, owing in part to disruption of tight junctions.[61-63] Furthermore, EMT is known to down-regulate tight junction components, including several members of the Claudin protein family.[64] Claudins are integral membrane proteins localized at tight junctions that are involved in regulating epithelial cell polarity and paracellular permeability. Intriguingly, previous data revealed that overexpression of miR-200 family members (which inhibit *ZEB1* expression) or direct exogenous silencing of ZEB1 has a protective effect in a murine, lipopolysaccharide-induced model of ARDS.[65] In this context, our findings support a novel model for the pathogenesis of SARS-CoV-2 in which the virus initially infects a small pool of highly epithelial cells of the aerodigestive and respiratory tracts followed by those infected cells undergoing molecular alterations typical of EMT (i.e., *ZEB1* or *AXL* up-regulation). These EMT-like alterations, in turn, result directly in the down-regulation of genes associated with tight junctions and, in doing so, eradicate the proposed ARDS-protective effect of these epithelial, ACE2-positive cells.

Materials and Methods

Transcriptional Sequencing Data Sets

RNA sequencing (RNAseq) analysis data sets from normal tissues were obtained from Genotype-Tissue Expression portal (http://www.gtexportal.org), and tumor samples were retrieved from published and unpublished data sets in multiple human tissues, including The Cancer Genome Atlas (TCGA) lung adenocarcinoma (LUAD),[11] TCGA head and neck squamous cell (tumors) (HNSC),[12] TCGA Lung Squamous Cell Carcinoma, PROSPECT,[13] BATTLE 1,[14] and BATTLE 2.[15] Cell line RNAseq data were obtained from multiple sources, including the Cancer Cell Line Encyclopedia upper aerodigestive tract (n = 32), LCNEC cell lines (n = 15),[16] NSCLC (n = 88),[17,18] head and neck squamous cell carcinoma (cell lines) (HNSCC) (n = 70),[19] and SCLC (n = 62).[66]

Transcriptional data from experimental data sets were publicly available, including EMT induction by 3 weeks of transforming growth factor-β (TGF-β),[20] 393P

murine cells with Zeb1 overexpression,[21] erlotinib resistance through EMT in *EGFR*-mutated HCC4006 and HCC827 NSCLC cell lines,[22] gefitinib-resistant PC-9 cells through EMT,[23] T790M-mediated gefitinib resistance in PC-9 cells,[24] and Calu-3 or A549 transduced with a vector-expressing human ACE2 that were mock infected or infected with SARS-CoV-2 (USA-WA1/2020),[25] forced miR-200 expression in 344SQ LUAD cells with high metastatic potential,[26] human bronchial organoids that were infected with SARS-CoV-2 for 5 days,[27] and nasopharyngeal swabs from patients with positive or negative SARS-CoV-2 polymerase chain reaction (PCR) results.[28]

Single-cell RNAseq (scRNAseq) data were obtained from publicly available sources, including bronchial epithelial cells obtained by bronchial brushings from six never smokers and six current smokers,[29] oral cavity tumors from 18 tumors,[30] five normal donor and eight fibrotic lungs,[31] freshly resected parenchymal lung tissue from three patients,[32] bronchial biopsy, nasal brushing, nasal turbinate specimens (GSE121600), and PC-9 *EGFR*-mutant NSCLC cell xenograft tumors treated with vehicle or osimertinib for 3 weeks.[33]

Chromatin immunoprecipitation sequencing analysis of ZEB1 binding in the *ACE2* promoter of HepG2, human hepatocyte carcinoma cells, was as previously described.[34]

Flow Cytometry

One million cells each for HCC2302, H3255, HCC827, H1944, H441, H2023, HCC364, A549, H1355, and HCC827 vectors and HCC827 ZEB1 were surfaced stained for ACE2 (Santa Cruz; sc-390851), fixed in 2 % perfluoroalkoxy alkanes, and permeabilized using 1× Intracellular Staining Perm Wash Buffer (BioLegend; 421002) before intracellular staining for vimentin (BD Pharmingen; 562338). The samples were analyzed on a BD LSRFortessa Flow Cytometer, and data were analyzed using FlowJo 10.7.1. Graphs and statistical analysis were done using GraphPad Prism 8.

Metabolite Assay

One million cells each for 393P ZEB1 (DMSO 16 h), 393P ZEB1 (DOX 16 h), H441, H1944, HCC2302, HCC827, H2023, and H1355 were harvested. Cell lysates were prepared by addition of 0.3 N hydrochloric acid and then 450 nM Tris (pH = 8), and metabolites were analyzed using the Glutamine/Glutamate Glo Assay (Promega; J8021) per manufacturer's instructions.

Drug Treatment of Cells

393P-Zeb1–inducible murine NSCLC cells were treated with AXL inhibitor, bemcentinib (0.5 μM), or DMSO for a total of 24 hours (8-h pretreatment with bemcentinib or DMSO, followed by induction of Zeb1 with doxycycline [2 μg/mL], and an additional 16-h drug treatment). Five NSCLC cell lines with varying levels of ACE2 were treated with hydroxychloroquine sulfate (Sigma) for 48 hours. Cell lysates were harvested for Western blot or reverse-phase protein array (RPPA) analysis. Antibodies used for Western analysis include ACE2 (MA5-32307, ThermoFisher), GLUL (80636, Cell Signaling Technology), Vimentin (3932, Cell Signaling Technology), ZEB1 (3396, Cell Signaling Technology), and vinculin (Sigma, V9131) as a loading control. The cell line drug-screening data were generated internally. Three measurements were performed for each drug at each concentration to produce dose-response data and determine concentration that inhibits 50 % value.

Reverse-Phase Protein Array

Protein lysates from TCGA LUAD, NSCLC cell lines, and Calu-1 or 393P cells treated with bemcentinib were quantified, and protein arrays were printed and stained.[67] Images were quantified with MicroVigene 4.0 (VigeneTech, Carlisle, MA). The spot-level raw data were processed with the R package SuperCurve suite, which returns the estimated protein concentration (raw concentration) and a quality control score for each slide, as described previously.[67] Only slides with a quality control score of greater than 0.8 were used for downstream analysis. The raw concentration data were normalized by median centering each sample across all the proteins to correct loading bias.

miRNA Arrays

Total RNAs from 55 NSCLC, 30 SCLC, and 49 HNSCC cell lines were analyzed with Affymetrix miRNA 4.0 arrays. The expression data of a curated list of miR-200 family members (hsa-miR-200b-5p, hsa-miR-200b-3p, hsa-miR-200c-5p, hsa-miR-200c-3p, hsa-miR-200a-5p, hsa-miR-200a-3p, hsa-miR-429, hsa-miR-141-5p, hsa-miR-141-3p) known to be involved with EMT in NSCLC[68] were compared with ACE2 expression data.

Metabolite Analyses

A total of 225 metabolites were profiled in the Cancer Cell Line Encyclopedia upper aerodigestive tract cell lines using liquid chromatography–mass spectrometry.[69] We compared *ACE2* mRNA expression to abundance of metabolites.

Computational Prediction of Binding Sites

To generate the predicted ZEB1 (E-Box) binding sites on the ACE2 promoter, the promoter sequence for human ACE2 was downloaded and used in the matrix

profile search on the JASPAR web portal.[70] For the search, the vertebrate database selecting ZEB1-binding motifs was selected to search through the promoter sequence of ACE2 with a relative profile threshold score cutoff of 80 % or higher. The resulting sites were ranked, and accordingly, the highest scoring motifs were annotated on the promoter segment using SnapGene.

scRNAseq Analysis

Raw data for single-cell datasets were downloaded from the Gene Expression Omnibus (GEO) database and processed using the Seurat Package version 2.3.1.[71] First, the raw read counts were normalized and scaled using "NormalizeData" and "ScaleData" function. The most variable genes were selected using the "FindVariableGenes" function with default parameters, and principle component analysis (PCA) was performed on these variable genes. We selected the first N principle components that account for at least 80 % of the total variances to perform the t-distributed stochastic neighbor embedding (tSNE) transformation. For each gene, the expression status is defined as positive if the cell has nonzero expression value, or negative otherwise. For GSE122960, samples were grouped to donor samples (including GSM3489182, GSM3489187, GSM3489189, GSM3489191, and GSM3489193) and fibrotic samples (including GSM3489183, GSM3489184, GSM3489188, GSM3489190, GSM3489192, GSM3489194, GSM3489196, and GSM3489198). Each group was subsampled to 20,000 total cells. EMT score was calculated on the basis of the EMT signature as described previously.[72,73] Cell-specific expression of *SFTPC* (alveolar type II cells), *FOXJI*, *PIFO* (ciliated cells), and *SCGB1A1* (club cells) was visualized in tSNE feature plots to identify epithelial clusters containing *ACE2*-positive cells.

Data Quality Assessments

Before performing any analyses, the data sets were screened for data quality. One example of a data set used in these analyses is the NCI TCGA, a landmark cancer genomics program that characterized more than 20,000 primary cancer and adjacent normal tissues from 33 different cancer types. These data are publicly available to the research community for the purpose of investigating novel hypotheses. RNAseq data were inspected for total read counts across all samples as a quality check for library size. Furthermore, datasets were excluded from our analyses owing to highly volatile total read counts. In both microarray and RNAseq data sets, PCA using all features was performed to make sure that no outlier samples were present. When distinct grouping information was included (i.e., control versus infected, positive versus negative), we performed PCA analysis to make sure that there was a good separation in the PCA plot. In addition to data quality assessments, we also considered sample size for each individual data set with a minimum of three samples per group required for further analyses.

The public microarray gene expression data were directly downloaded in the original processed data format from the GEO site. For scRNAseq data, we used the read counting and unique molecular identifier count data matrices in GEO. No additional data-filtering steps were applied. All the TCGA data used were level 3 processed data. Data quality across data sets is not comparable and contains considerable batch effects, especially with the use of different technologies. Therefore, data sets were not combined and all analyses were performed on individual data sets.

Statistical Analyses

All statistic and bioinformatics analyses were performed using R. Paired and unpaired two-sample *t* tests were used for two-group comparisons on paired and unpaired experimental design experiments. Pearson and Spearman correlations were used for correlating genomic and proteomic measurements, including correlating drug-screening data. In all the analyses, *p* value less than 0.05 was considered statistically significant.

The drug-target constellation map was generated on the basis of drug-screening data using a suite of R packages, including ggplot2, ggraph, and igraph. A list of drugs was selected on the basis of Spearman coefficient (>0.3) and *p* value (<0.1), and only targets with more than five associated drugs were revealed in the figure.

Data Set Availability

Publicly available data were obtained from the following GEO data sets: GSE122960, GSE131391, GSE103322, GSE42127, GSE122960, GSE130148, GSE138693, GSE121600, GSE49644, GSE61395, GSE114647, GSE75602, GSE147507, GSE15741, GSE150819, GSE154770, and GSE32465 (GSM1010809).

Results

Expression of ACE2 by Cancer Epithelial Cells

Data sets from multiple sources were used in these analyses, including those publicly available in GEO data sets and those generated by our laboratory, department, and the longstanding joint The University of Texas Southwestern/MD Anderson Cancer Center NCI Lung SPORE program.[11-34] The publicly available data include sets such as TCGA, an NCI resource established for data discovery and hypothesis testing. A rigorous analysis of data quality was performed before inclusion. No comparisons were made across data sets. None of the

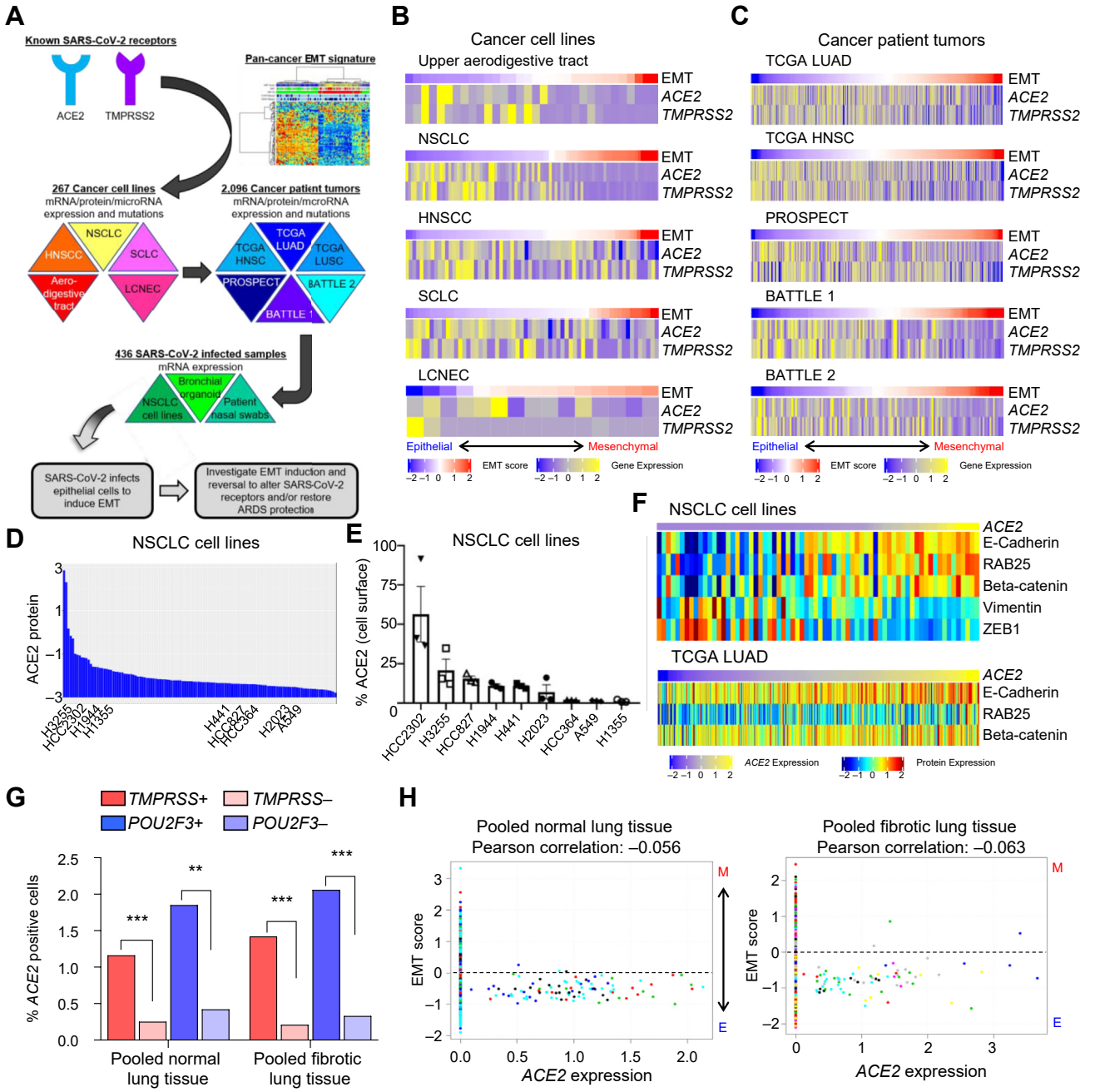

Figure 1. The SARS-CoV-2 receptor, *ACE2*, is expressed by epithelial cells in cancer models. (*A*) Schematic depicting an overview of the strategy to investigate ACE2 biology in the context of EMT using cancer cell lines and tumor samples before applying to SARS-CoV-2–infected samples to develop our hypotheses. (*B*) *ACE2* and *TMPRSS2* expression and EMT score in aerodigestive and lung cancer cell lines (*ACE2* versus EMT score, $p < 0.0001$ for all) and (*C*) in patient tumor biopsies (*ACE2* versus, EMT score, $p < 0.0001$ for all). TCGA sets (LUAD and HNSC) refer to LUAD and HNSCC, respectively. The BATTLE-1, BATTLE-2, and PROSPECT trials include only NSCLC. Rho values are listed in Table 1. (*D*) ACE2 protein levels in NSCLC cell lines. (*E*) Cell surface ACE2 in a subset of NSCLC cell lines. (*F*) NSCLC cell lines and TCGA LUAD tumor biopsies were ranked by *ACE2* mRNA expression and reveal protein expression of common epithelial (E-cadherin, RAB25, beta-catenin) or mesenchymal (vimentin, ZEB1, fibronectin) markers. (*G*) Frequency of *ACE2*-positive cells in *TMPRSS2*-positive or -negative cells and *POU2F3*-positive or negative cells as determined by single-cell RNAseq of donor or fibrotic lungs. (*H*) EMT score values for each *ACE2*-positive cell present in five donor and eight fibrotic lungs. Each colors represent cells from an individual lung sample. $^{**}p < 0.01$, $^{***}p < 0.001$. ARDS, acute respiratory distress syndrome; EMT, epithelial-to-mesenchymal transition; HNSC, head and neck squamous cell (tumors); HNSCC, head and neck squamous cell carcinoma (cell lines); LCNEC, large cell neuroendocrine carcinoma; LUAD, lung adenocarcinoma; RNAseq, RNA sequencing; SARS-CoV-2, severe acute respiratory syndrome coronavirus 2.

Table 1. ACE2 Rho Correlation Values in Aerodigestive and Respiratory Tract Cell Line and Tumor Biopsy Specimens

Dataset	*TMPRSS2*	*POU2F3*	EMT Score	*ZEB1*	*AXL*	*GLUL*	*GLS*
NSCLC cell lines	0.565[a]	0.668[a]	−0.694[a]	−0.801[a]	−0.410[a]	0.394[a]	−0.202[b]
HNSCC cell lines	0.230[b]	0.188	−0.408[a]	−0.388[a]	−0.078	0.306[c]	−0.042
SCLC cell lines	0.069	0.394[c]	−0.401[a]	−0.429[a]	−0.351[b]	0.284[b]	−0.305[b]
TCGA LUAD	0.228[a]	0.328[a]	−0.286[a]	−0.28[a]	−0.083	0.296[a]	−0.197[a]
TCGA HNSC	0.082	0.159[a]	−0.402[a]	0.238[a]	−0.239[a]	0.037	−0.071
TCGA LUSC	0.242[a]	0.033	−0.239[a]	−0.070	−0.121[c]	0.404[a]	−0.179[a]
PROSPECT	0.195[a]	0.065	−0.279[a]	−0.117[b]	−0.090[c]	−0.091	0.126[b]
BATTLE 1	0.437[a]	0.134	−0.367[a]	−0.166[b]	−0.222[c]	0.339[a]	−0.082
BATTLE 2	0.373[a]	0.249**	−0.337[a]	−0.196[b]	−0.235[c]	0.208[c]	−0.064

[a]*p* value less than 0.001.
[b]*p* value less than 0.05.
[c]*p* value less than 0.01.
HNSC, head and neck squamous cell (tumors); HNSCC, head and neck squamous cell carcinoma (cell lines); LUAD, lung adenocarcinoma; LUSC, lung squamous cell carcinoma; TCGA, The Cancer Genome Atlas.

comparisons or queries were previously performed or published.

ACE2 is widely expressed in normal tissues from Genotype-Tissue Expression Project (http://www.gtexportal.org) and was highest in testis and small intestine and lowest in spleen and blood with moderate expression in lung and salivary glands, which are sites of SARS-CoV-2 transmission or infection (Supplementary Fig. 1*A*). Transcriptional data are revealed as normalized relative gene expression.

To leverage cancer cell lines and patient tumors to SARS-CoV-2 research, we explored expression of the receptors, *ACE2* and *TMPRSS2*, and discovered a negative correlation with EMT. This was validated in SARS-CoV-2–infected samples and led to investigation of ways to manipulate EMT in an effort to minimize infection or ARDS in patients (Fig. 1*A*). *ACE2* expression in aerodigestive and respiratory cancer cell lines (Fig. 1*B*) and both normal and tumor specimens (Fig. 1*C*) is consistently higher in specimens with a low EMT score, suggesting *ACE2* is primarily expressed by epithelial cells in these cancers.[11-19,66,74,75] The EMT score uses 76 genes to define the degree to which cells or tissues have undergone EMT and has been applied in TCGA projects.[72,76,77] This observation is confirmed by a consistent negative correlation of *ACE2* and EMT score in all nine cell line and tumor data sets (Table 1). *TMPRSS2*, the protease also required for SARS-CoV-2 infection, is similarly expressed in models with epithelial gene signatures (Fig. 1*B* and *C*) and highly correlated with *ACE2* expression in cancer models (Table 1). To determine whether expression levels of *ACE2* were different in normal tissues and tumors, we compared expression in TCGA tumor data sets with paired normal, adjacent samples. Both normal and LUAD tissues have similar *ACE2* expression (TCGA LUAD $p = 0.21$) and EMT score (TCGA LUAD $p = 0.87$) (Supplementary Fig. 1*B*), although a greater range of expression (both higher and lower) could be observed in tumors.[78-80] Interestingly, and in contrast to some previous reports, no difference in *ACE2* expression was detected in normal lung tissue (adjacent to TCGA LUAD) with regard to smoking status, gender, or age (Supplemental Fig. 1*C*).

In addition to *ACE2* mRNA expression, we screened a cohort of NSCLC and SCLC cell lines for ACE2 protein levels by RPPA (Fig. 1*D*), and within a subset of NSCLC cell lines, we analyzed cell surface expression of NSCLC cell lines by flow cytometry (Fig. 1*E*). Similar to gene expression, ACE2 levels negatively correlate with mesenchymal proteins, including vimentin (Supplemental Fig. 1*D*). To go beyond the quantitative, gene-based EMT score, we investigated expression of

Table 2. Total Number of *ACE2*-Positive Cells and EMT Score

Data Sets	Total No. of Cells/Samples	*ACE2*+ Cells (%)	EMT Score in *ACE2*+ Cells
Bronchial brushings (GSE131391)	1146 cells (12 patients)	54 (4.71)	−0.13
Oral cavity tumors (GSE103322)	5902 cells (18 tumors)	87 (1.47)	−0.54
Donor lungs (GSE122960)	20,000 cells (5 lungs)	94 (0.47)	−0.52
Fibrotic lungs (GSE122960)	19,587 cells (8 lungs)	72 (0.37)	−0.75
Parenchymal lung (GSE130148)	10,360 cells (3 lungs)	14 (0.14)	−0.26
PC9 xenograft DMSO treated (GSE138693)	3766 cells (1 xenograft)	29 (0.77)	−0.40
PC9 xenograft osimertinib treated (GSE138693)	2332 cells (1 xenograft)	0 (0)	N/A
Bronchial biopsy/nasal brushing/turbinate (GSE121600)	12,000 cells (3 specimens)	4 (0.03)	−0.49

EMT, epithelial-to-mesenchymal transition; N/A, not applicable.

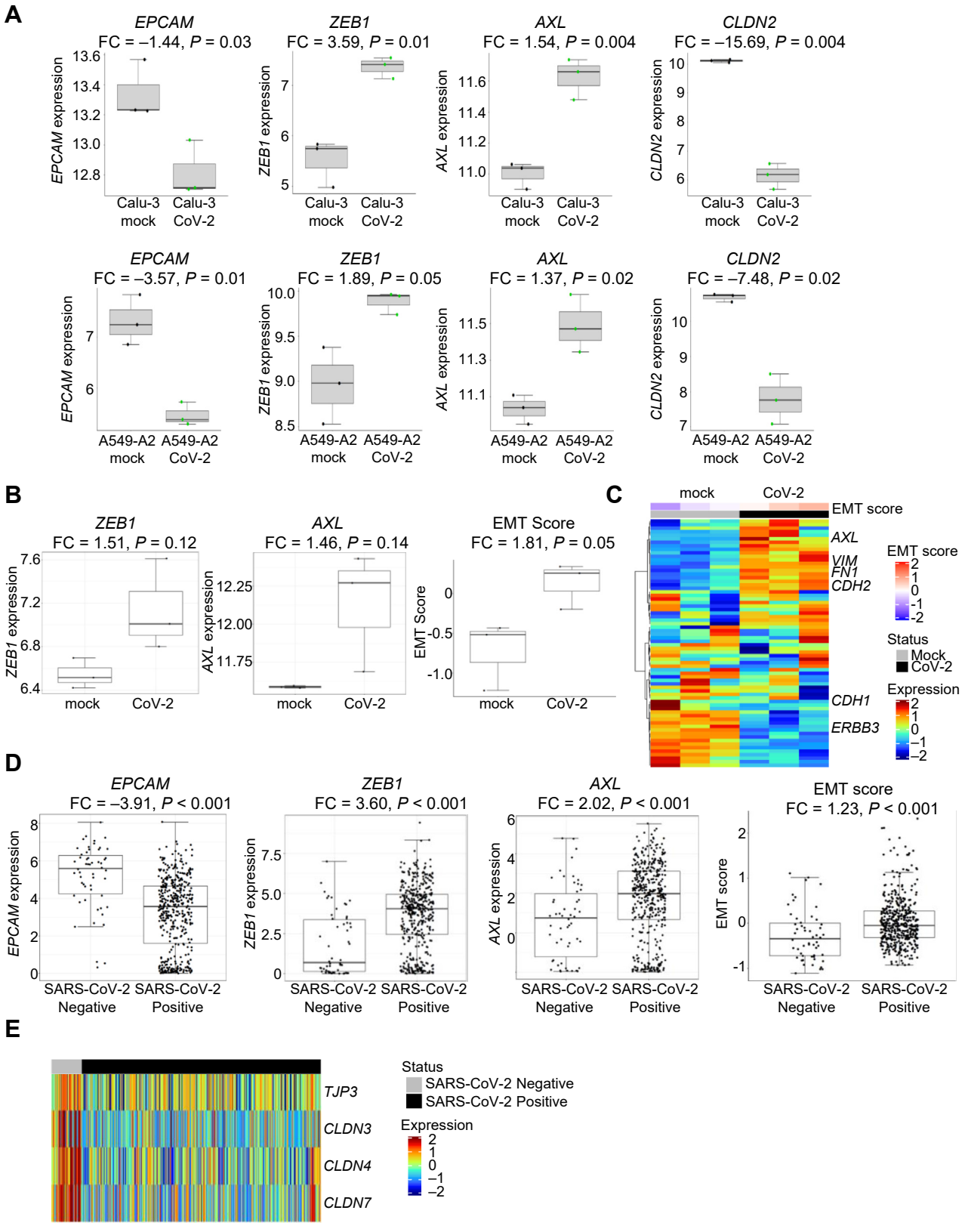

Figure 2. SARS-CoV-2 induces EMT. (*A*) Effects of SARS-CoV-2 infection of Calu-3 or A549+ACE2 for 24 hours on *EPCAM*, *ZEB1*, *AXL*, and *CLDN2* expression. (*B*) Effects of SARS-CoV-2 infection on human bronchial organoids for 5 days on *ZEB1* and *AXL* expression and EMT score. (*C*) Heatmap revealing differences in gene expression between mock and SARS-CoV-2–infected bronchial organoids in EMT-associated genes. (*D*) Effects of SARS-CoV-2 infection in nasal swab samples from 430 individuals with PCR-confirmed SARS-CoV-2 and 54 negative controls on *EPCAM*, *ZEB1*, *AXL* expression and EMT score. (*E*) Effects of

ACE2 mRNA compared with specific epithelial (i.e., E-cadherin, RAB25, beta-catenin) or mesenchymal (i.e., vimentin, ZEB1) proteins by RPPA analysis. *ACE2* was higher in NSCLC cell lines ($p < 0.008$) and TCGA tumors ($p < 0.001$; Fig. 1*F*) with higher levels of epithelial proteins, consistent with the mRNA associations and EMT score.

Our analyses reveal that *ACE2* is only expressed by a small subset of cells (0%–4.7 %) at the single-cell transcriptional level in normal respiratory tissues, including in oral cavity tumors and lung cancer xenograft models (Table 2).[30-33,81] Nevertheless, in all data sets, the rare, *ACE2*-positive cells consistently have a low, or more epithelial, EMT score. In both fibrotic and donor lung samples, *TMPRSS2* is more widely expressed than *ACE2*, whereas *ACE2* expression is found more frequently in *TMPRSS2*-positive cells (Fig. 1*G* and Supplementary Table 1) relative to *TMPRSS2*-negative cells. As studies suggest that both are required for infection, these data indicate that *ACE2* expression is more limiting than *TMPRSS2* expression for SARS-CoV-2 infection within respiratory epithelium.

POU2F3 is a marker of tuft cell expression and is correlated with *ACE2* expression in many aerodigestive and lung cancer data sets (Table 1). ACE2 protein levels also correlate with POU2F3 in both NSCLC (Rho = 0.221, $p = 0.01$) and SCLC (Rho = 0.673, $p < 0.0001$) cell lines. Similar to the observation for co-expression with *TMPRSS2*, *ACE2* expression is more often detected in *POU2F3*-positive than -negative cells (Fig. 1*G* and Supplementary Table 1). This suggests that tuft cells may be preferentially targeted by SARS-CoV-2 infection in aerodigestive tissues. These rare, *ACE2*-positive cells can be visualized in tSNE space (Supplemental Fig. 2*A*) and had a low EMT score on a cell-by-cell basis in both donor and fibrotic lung samples (Fig. 1*H*) and oral cavity tumors (Supplemental Fig. 2*B*). These *ACE2*-positive cells are localized within epithelial cell clusters with low EMT score that primarily consist of alveolar type II ciliated and club cells (Supplemental Fig. 2*C*) on the basis of expression of cell-type specific markers including *SFTPC* (alveolar type II cells), *FOXJI* (ciliated cells), and *SCGB1A1* (club cells).

SARS-CoV-2 Infection Induces EMT

We next sought to reveal the impact of SARS-CoV-2 infection on the EMT status of the infected cell. We analyzed RNAseq data from NSCLC cell lines (A549 and Calu-3) infected for 24 h with SARS-CoV-2 (GSE147507).[25] These are cell lines that are frequently used for lung cancer research. Because A549 cells have low endogenous levels of *ACE2* expression, likely owing to their mesenchymality, the authors also transduced these cells with a vector overexpressing human ACE2 to improve infection. Expression of the epithelial gene *EPCAM* was down-regulated after viral infection (Calu-3, $p = 0.03$, A549+ACE2, $p = 0.01$, Fig. 2*A*; A549, $p = 0.04$, Supplemental Fig. 3*A*), suggesting infection is inducing a shift away from an epithelial phenotype. This was confirmed by *ZEB1* up-regulation in all three cell lines (Calu-3, $p = 0.01$, A549+ACE2, $p = 0.05$, Fig. 2*A*; A549, $p = 0.003$, Supplementary Fig. 3*A*) after infection.

An alternative EMT regulator, AXL, which is a TAM (Tyro3, AXL, Mer) family receptor tyrosine kinase strongly associated with a mesenchymal phenotype, has emerged as a key determinant of therapeutic resistance in NSCLC and other cancer types.[72,82] Similar to *ZEB1*, *AXL* is inversely correlated with *ACE2* in cell line and tumor samples (Table 1). Furthermore, infection of cells with SARS-CoV-2 up-regulated *AXL* expression in all three cell lines (Calu-3, $p = 0.004$, A549+ACE2 $p = 0.02$, Fig. 2*A*; A549, $p < 0.001$, Supplementary Fig. 3*A*). A similar induction of mesenchymal genes with viral infection was observed for *SNAI1* (Calu-3: fold change [FC] = 1.84, $p = 0.009$; A549+ACE2: FC = 7.43, $p = 0.01$) and *ZEB2* (Calu-3: FC = 6.74, $p = 0.002$; A549+ACE2: FC = 5.17, $p = 0.0001$). Nevertheless, EMT score was not different between mock- or SARS-CoV-2–infected Calu-3 (FC = −1.09, $p = 0.14$) or A549+ACE2 cells (FC = −1.03, $p = 0.48$), and this may be due to the relatively short period of viral infection (24 h).

We next investigated whether SARS-CoV-2 infection directly altered Claudin expression. *CLDN2* is expressed in respiratory epithelium, but a role in mediating alveolar edema has not been described.[83] Nevertheless, of all Claudin family members, *CLDN2* was down-regulated in all three cell lines (Calu-3, $p = 0.004$, A549+ACE2, $p = 0.02$ Fig. 2*A*; A549, $p = 0.008$, Supplemental Fig. 3*A*), suggesting a change in epithelial and endothelial cell permeability that may contribute to ARDS in patients with COVID-19. Similarly, there was a reduction in *TJP3*, the gene encoding a scaffolding protein that links tight junction transmembrane proteins, such as claudins, to the actin cytoskeleton (Calu3: FC = −1.48, $p = 0.04$; A549+ACE2: FC = −2.89, $p = 0.10$) after viral infection. Evidence of a metabolic shift away from glutamine was observed postinfection, as *GLUL* expression was reduced in *ACE2*-high cell lines, but not in non-transfected A549 (Calu-3 $p = 0.01$, A549+ACE2

SARS-CoV-2 infection in nasal swabs on genes associated with tight junctions. RNAseq data are revealed as normalized relative gene expression. CoV-2, coronavirus 2; EMT, epithelial-to-mesenchymal transition; FC, fold change; PCR, polymerase chain reaction; RNAseq, RNA sequencing; SARS-CoV-2, severe acute respiratory syndrome coronavirus 2.

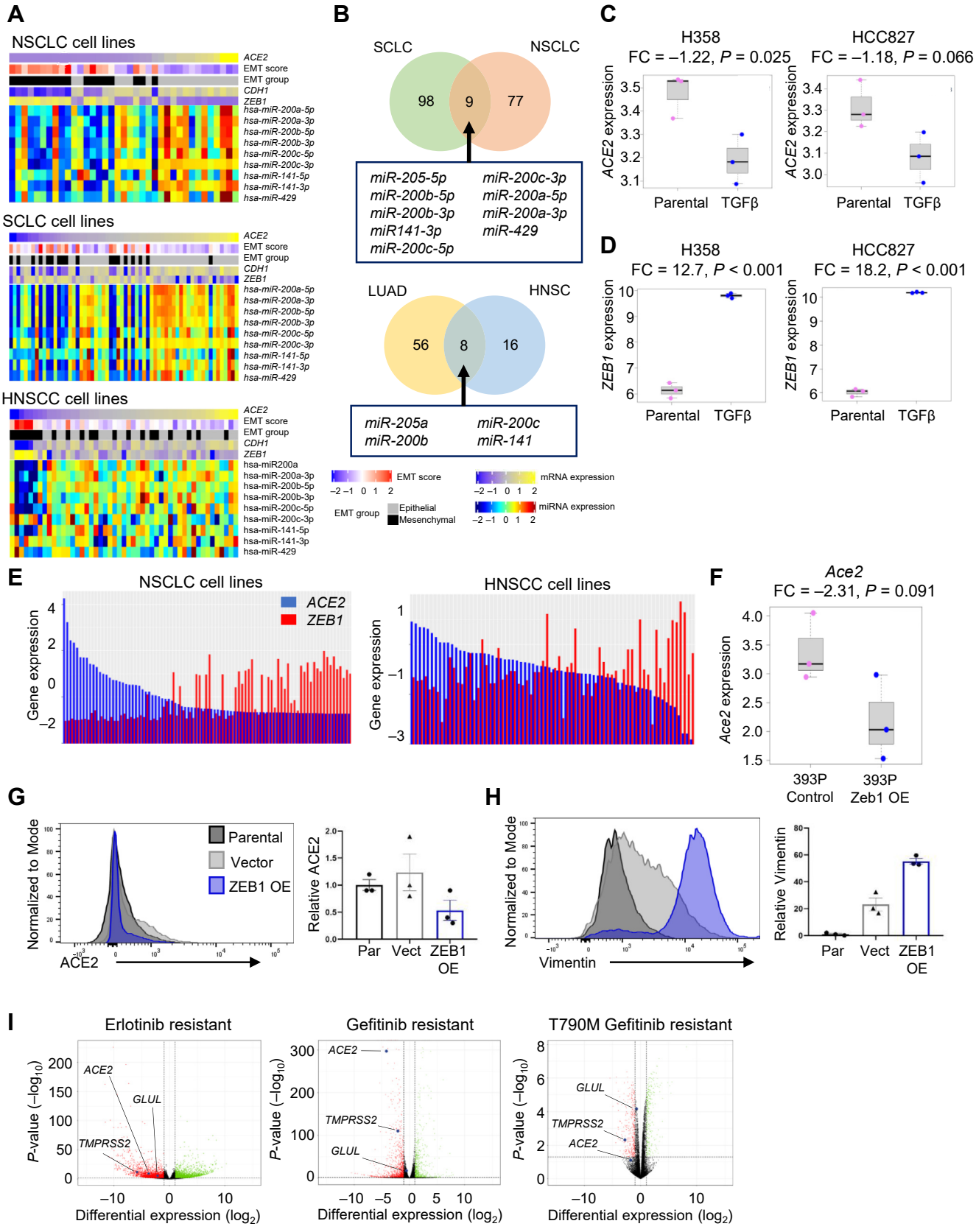

Figure 3. *ACE2* repression by EMT in lung cancer cells. (*A*) *ACE2*, EMT score, EMT group (epithelial or mesenchymal), *CDH1*, and *ZEB1* expression with miR200 family miRNAs in NSCLC, SCLC, and HNSCC cell lines. (*B*) Venn diagrams revealing miRNAs correlated with *ACE2* expression in both NSCLC and SCLC cell lines (upper) and TCGA LUAD and HNSC tumor biopsies (lower).

$p = 0.01$, Supplemental Fig. 3*B*, A549, $p = 0.56$). The *ZEB1* and *AXL* increase and *EPCAM* and *GLUL* decrease point toward a SARS-CoV-2–induced shift from an epithelial to a mesenchymal phenotype.

To reveal whether longer exposure to virus may induce additional EMT changes, we analyzed RNAseq data from human bronchial organoids developed from commercially available, cryopreserved adult bronchial epithelial cells infected with SARS-CoV-2 for 5 days (GSE150819).[27] There was a subtle increase in both *ZEB1* ($p = 0.12$) and *AXL* ($p = 0.14$) and other mesenchymal genes, including *VIM* (FC = 1.56, $p = 0.01$), *ZEB2* (FC = 3.23, $p = 0.22$), *SNAI1* (FC = 4.75, $p = 0.05$), and *CDH2* (FC = 2.06, $p = 0.02$). Importantly, longer SARS-CoV-2 infection increased the EMT score ($p = 0.05$; Fig. 2*B*). Although these shifts are not as strong as those found in the cell lines, there is a clear pattern for expression of the epithelial and mesenchymal genes making up the EMT score by heatmap (Fig. 2*C*). Similar to the NSCLC cell lines, SARS-CoV-2 infection down-regulated expression of tight junction-related genes, including *CLDN8* (FC = −2.66, $p = 0.009$) and *CLDN17* (FC = −1.62, $p = 0.05$).

Finally, to evaluate whether viral-induced EMT also occurs in patients, we analyzed metagenomic next-generation sequencing data of human nasopharyngeal swabs from 430 PCR-confirmed SARS-CoV-2 and 54 negative control individuals (GSE154770).[28] SARS-CoV-2 infection down-regulated expression of EPCAM ($p < 0.0001$) and up-regulated *ZEB1* ($p < 0.0001$) and *AXL* ($p < 0.0005$; Fig. 2*D*). Similar patterns were found with other epithelial genes, including *RAB25* (FC = −2.35, $p < 0.0001$) and *CTNNB1* (FC = −3.38, $p < 0.0001$), or mesenchymal genes, including *ZEB2* (FC = 8.14, $p < 0.0001$). As expected, viral infection was associated with an increased EMT score ($p < 0.0001$; Fig. 2*D*) and *TGFB1* expression (FC = 2.75, $p < 0.0001$). Interestingly, EMT gene expression was not affected by viral load (Supplemental Fig. 3*C*), as defined by the cycle threshold of the SARS-CoV-2 nucleocapsid gene region 1 (N1) target during diagnostic PCR.[28] This suggests that EMT is induced in cells, regardless of the viral burden in the patient. Consistent with the previous metabolic data, SARS-CoV-2 infection induces expression of *GLS*, indicating a shift away from glutamine production ($p = 0.009$; Supplemental Fig. 3*D*). Similar to the cell lines and bronchial organoids, SARS-CoV-2 infection reduces expression of genes associated with tight junctions (Fig. 2*E*), including *CLDN4* (FC = −6.63, $p < 0.0001$), *CLDN7* (FC = −6.59, $p < 0.0001$), *CLDN3* (FC = −5.14, $p < 0.0001$), *CLDN9* (FC = −1.72, $p < 0.0001$), *CLDN23* (FC = −1.95, $p = 0.0002$), *TJP2* (FC = −1.58, $p = 0.05$), and *TJP3* (FC = −2.22, $p < 0.0001$).

Induction of EMT Represses ACE2 Expression

To connect differences in *ACE2* expression to a more specific EMT regulatory program, we investigated miRNAs in both lung cancer and head and neck cell lines and tumor samples. Interestingly, miRNAs from the miR-200 family were consistently positively correlated with *ACE2*.[68] As expected, given their known role as inhibitors of EMT, high miR-200 family expression was found in cells and tumors with high *CDH1* (an epithelial-specific marker) and low EMT score and *ZEB1*, the latter a transcriptional promoter of EMT and target of miR-200 family (Fig. 3*A* and Supplementary Fig. 3*E*). The miR-200 family was correlated with *ACE2* expression in NSCLC,[21] SCLC, and HNSCC cell lines ($p < 0.01$; Fig. 3*B* and Supplementary Fig. 3*E*)[84] and both TCGA LUAD and HNSC tumors (Fig. 3*B*). Nevertheless, forced miR-200 expression in 344SQ LUAD cells with high metastatic potential was not sufficient to alter *ACE2* expression (Supplementary Fig. 3*F*).[26] miR-200 family members repress *ZEB1* expression, so unsurprisingly *ACE2* is negatively correlated with *ZEB1* in cancer cell lines and tumors (Table 1). *ACE2* similarly is negatively correlated with a number of other EMT-associated genes, including *ZEB2*, *SNAI1*, *SNAI2*, *TWIST1*, and *CDH2* (Supplementary Table 2). Although these correlations are almost invariably negative, as expected, none of these genes reveal a negative correlation as robust and consistent across data sets between *ACE2* as EMT score or *ZEB1.*

To reveal whether transformation from an EMT directly alters *ACE2* expression, we used various methods to induce EMT, including treatment with TGFβ, overexpression of ZEB1, and EGFR tyrosine

RNAseq data are revealed as normalized relative gene expression. (*C*, *D*) Expression of (*C*) *ACE2* and (*D*) *ZEB1* after induction of EMT by TGF-β treatment in H358 and HCC827 NSCLC cell lines. (*E*) Expression of *ACE2* and *ZEB1* in NSCLC and HNSCC cell lines. (*F*) Expression of Ace2 in 393P murine lung adenocarcinoma cells with Zeb1 overexpression. Cell surface expression of (*G*) ACE2 and (*H*) Vimentin in HCC827 cells with constitutive overexpression of ZEB1. (*I*) *ACE2*, *TMPRSS2*, and *GLUL* expression in NSCLC cell lines with acquired resistance to EGFR TKIs that occurred through EMT but not when resistance occurred through EGFR T790M resistance mutations. RNAseq data are revealed as normalized relative gene expression. EMT, epithelial-to-mesenchymal transition; FC, fold change; HNSC, head and neck squamous cell (tumors); HNSCC, head and neck squamous cell carcinoma (cell lines); LUAD, lung adenocarcinoma; miRNA, microRNA; OE, overexpressing; Par, parental; RNAseq, RNA sequencing; TCGA, The Cancer Genome Atlas; TGF-β, transforming growth factor-β; TKI, tyrosine kinase inhibitor; Vect, vector.

kinase inhibitor (TKI) resistance. Two highly epithelial NSCLC cell lines cultured with TGFβ for 3 to 5 weeks[20] increased the EMT score (Supplemental Fig. 4*A*). Induction of EMT resulted in a loss of *ACE2* in H358 and HCC827 ($p = 0.03$ and $p = 0.06$, respectively; Fig. 3*C*). In addition, both cell lines exhibited increased *ZEB1* after EMT induction ($p < 0.0001$; Fig. 3*D*). The experiment also included EMT induction in A549 cells, but this line is more mesenchymal with low endogenous *ACE2* expression at baseline and TGFβ was unable to reduce already minimal *ACE2* ($p = 0.23$, data not found).

Accordingly, NSCLC and HNSCC cell lines reveal an inverse correlation between *ACE2* and *ZEB1* (Fig. 3*E*). Computational investigation of the *ACE2* promoter using the JASPAR database revealed five putative ZEB1 binding sites, suggesting ZEB1 may directly repress *ACE2* expression.[70] Two of these predicted binding sites (ZEB1-EBOX3, ZEB1-EBOX4) were confirmed by chromatin immunoprecipitation sequencing to be functional binding sites for ZEB1 in the *ACE2* promoter in HepG2, a hepatocellular cell line (Supplemental Fig. 4*B*). Consistent with this, induction of EMT by means of overexpression of Zeb1 in 393P murine LUAD cells results in a more than twofold reduction in *Ace2* expression ($p = 0.091$; Fig. 3*F*).[21] Furthermore, constitutive overexpression of ZEB1 in HCC827 cells[21,85,86] reduced cell surface expression of ACE2 compared with either the parental cell line ($p = 0.05$) or the vector control ($p = 0.07$; Fig. 3*G*). As expected, overexpression of ZEB1 increased vimentin levels (compared with parental, $p < 0.0001$, or vector control, $p = 0.002$; Fig. 3*H*). ACE2 is repressed by EMT, and this is mediated, at least in part, by ZEB1.

EGFR-mutated NSCLCs are routinely and effectively treated with EGFR TKIs, but resistance inevitably develops by means of characteristic mechanisms, including secondary *EGFR* resistance mutations (i.e., T790M) and, notably, EMT.[87] Thus, we evaluated expression of *ACE2* in *EGFR*-mutated NSCLC cells (HCC4006 and HCC827) treated with the EGFR TKI erlotinib until resistance occurred.[22] *ACE2* and *TMPRSS2* were down-regulated in EGFR TKI-resistant lines that had undergone EMT in comparison to parental (EGFR TKI-sensitive cells) (Fig. 3*I*). Separately, PC-9 cells, which also harbor *EGFR*-activating mutations and display high baseline levels of *ACE2*, were treated with the EGFR TKI gefitinib for 3 weeks until resistance emerged through EMT[23] or acquired T790M resistance mutations.[24] *ACE2* was down-regulated in gefitinib-resistant cells that had undergone an EMT but not in T790M+-resistant cells that maintained an epithelial phenotype (Fig. 3*I*). These findings are consistent with the notion of *ACE2* repression by the EMT regulator, ZEB1. In xenograft models, mice bearing PC-9 xenograft tumors treated with vehicle or the EGFR TKI osimertinib for 3 weeks to induce resistance through the EMT were transcriptionally profiled by scRNAseq.[33] *ACE2* was only detectable in vehicle-treated tumor cells, suggesting *ACE2* expression was lost in tumors that had undergone EMT.

Metabolic Signifiers of ACE2-Positive Cells

To identify metabolic features of cells able to be infected by SARS-CoV-2, metabolites associated with *ACE2* expression were investigated. *ACE2* expression correlates with glutamine in upper aerodigestive tract cell lines ($p < 0.01$; Supplemental Fig. 4*D*),[69] and ACE2 levels correlate with glutamine in a subset of NSCLC cell lines (rho = 0.89, $p = 0.02$; Supplementary Fig. 4*E*). Consistent with this finding, *ACE2* expression correlation with a list of 253 metabolism-associated genes and *GLUL*, which encodes an enzyme (glutamine synthetase) responsible for conversion of glutamate to glutamine, was identified in NSCLC, HNSCC, and SCLC cell lines (Supplementary Fig. 4*F*) and was confirmed in the tumor data sets (Table 1). In addition to *GLUL*, *DERA* and *SLC6A14* were identified and are implicated in nucleotide metabolism and amino acid (including glutamine) transport, respectively (Supplemental Fig. 4*F*). Interestingly, *GLS*, which encodes the enzyme (glutaminase) that catalyzes the opposing reaction, in which glutamine is converted to glutamate, is negatively correlated with *ACE2* expression (Table 1). Next, we evaluated whether ZEB1 is a regulator of metabolism. Unlike *Ace2*, Zeb1 is unable to directly regulate *Glul* expression in murine 393P cells overexpressing Zeb1 ($p = 0.23$, Supplementary Fig. 4*G*). This was confirmed by *ZEB1* gene silencing and overexpression analyses (data not found), suggesting the metabolic changes are not directly controlled by ZEB1. Interestingly, *GLUL* was down-regulated in EGFR TKI gefitinib-resistant cells that had undergone an EMT but not in T790M+-resistant cells that maintained an epithelial phenotype. (Fig. 3*I*). Similarly, *GLUL* expression was reduced after osimertinib resistance that occurred through the EMT (Supplementary Fig. 4*C*). Taken together, glutamine synthetase-catalyzed conversion of glutamate to glutamine in epithelial cells aims to increase production of amino acids and nucleotides, whereas in mesenchymal cells, glutaminase converts glutamine to glutamate to preferentially shift toward the tricarboxylic acid cycle, thus priming epithelial cells for viral infection.

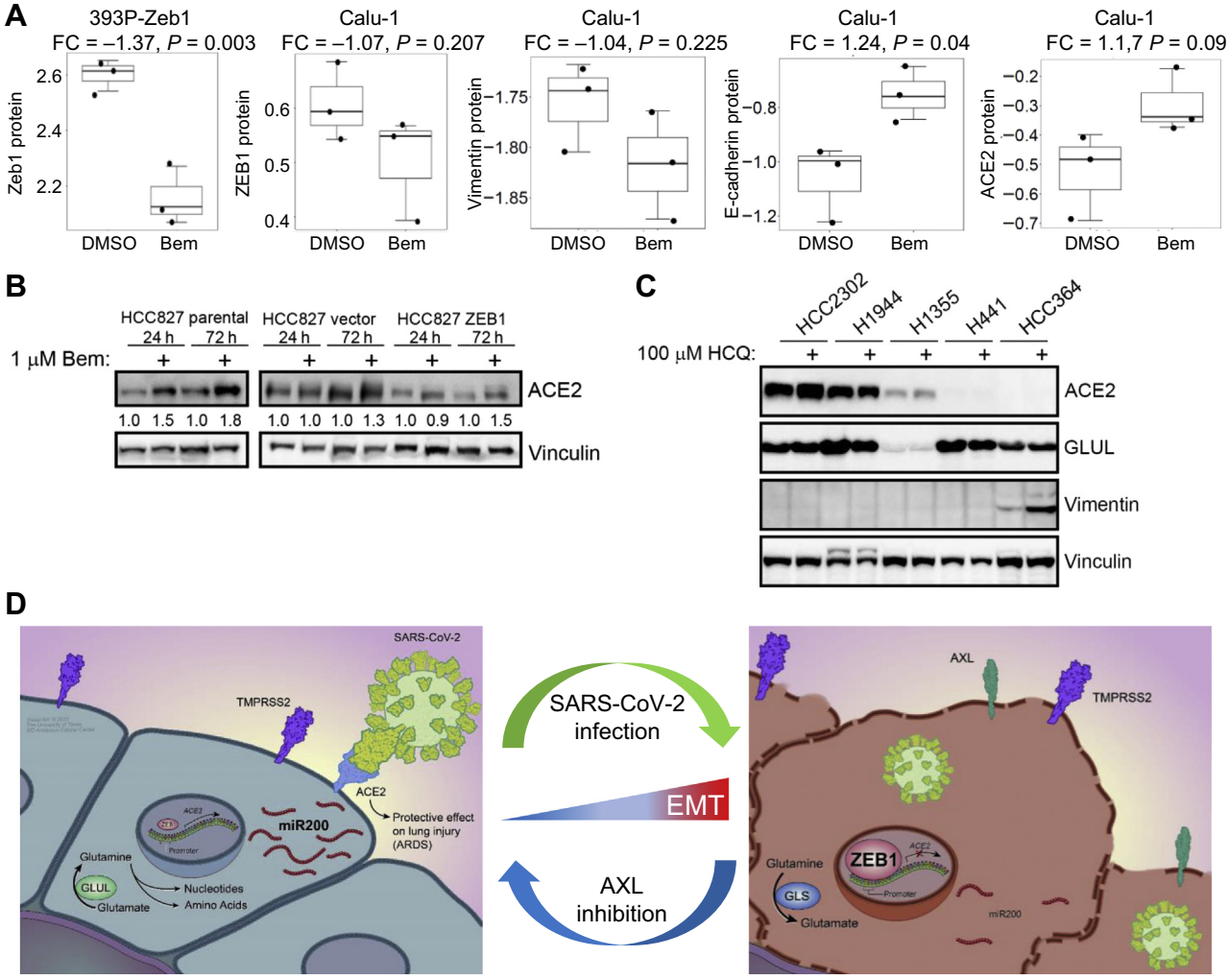

Figure 4. EMT modulation for treatment of SARS-CoV-2. (*A*) ZEB1 expression after 24 h of 0.5 μM Bem treatment in mesenchymal Calu-1 cells or after overexpression of Zeb1 in 393P murine cells, including vimentin, E-cadherin, and ACE2 in Calu-1 cells. (*B*) ACE2 levels after 24 h and 72 of 1 μM Bem treatment in HCC827 cells with constitutive overexpression of ZEB1. (*C*) ACE2, GLUL, and Vimentin levels in a subset of NSCLC cell lines after 48 h treatment with 100 μM hydroxychloroquine. (*D*) Working model revealing aerodigestive/respiratory cells with ACE2 expression are epithelial and metabolically primed for replication (left), whereas infected cells reveal a shift to a mesenchymal phenotype with reversal of glutamine production, a leaky cell membrane, and increased ZEB1 to induce EMT (right). ARDS, acute respiratory distress syndrome; Bem, bemcentinib; EMT, epithelial-to-mesenchymal transition; FC, fold change; h, hour; SARS-CoV-2, severe acute respiratory syndrome coronavirus 2.

EGFR/HER Family Link to ACE2

NSCLC encompasses a heterogeneous group of lung cancers with unique molecular features. To determine whether any previously characterized NSCLC subsets were linked to differential *ACE2* expression, we compared common driver mutation subsets of the TCGA LUAD tumors and found that *EGFR*-mutant LUAD tumors had significantly higher *ACE2* expression ($p = 0.001$; Supplemental Fig. 4*H*). *EGFR*-mutated tumors have constitutive activation of the EGFR and downstream signal transduction pathway. Accordingly, higher *ACE2* expression was associated with increased sensitivity to EGFR TKIs, as visualized by drug-target constellation map (Supplemental Fig. 3*I*). Moreover, *ACE2* expression was broadly correlated with increased expression of several EGFR/HER family members, including *EGFR*, *ERBB2*, and *ERBB3* in cell lines and tumors (Supplemental Fig. 3*J*), consistent with its preferential expression in epithelial cells. A similar link between EGFR inhibition and patients with COVID-19 has been described previously.[88]

Reversal of EMT

We hypothesized that bemcentinib (BGB324, or R428), an inhibitor of the mesenchymal receptor tyrosine kinase AXL with a known antiviral effect, may offer therapeutic benefit through a reversal of EMT.[89]

Bemcentinib down-regulated ZEB1 expression in mesenchymal cell lines, 393P overexpressing Zeb1 ($p = 0.003$) and Calu-1 ($p = 0.21$) (Fig. 4*A*). In Calu-1 cells, bemcentinib also down-regulated vimentin and up-regulated both E-cadherin and ACE2. Similarly, 48 hours of bemcentinib treatment in HCC827 parental, vector control, and ZEB1-constitutive overexpressing lines[21,85,86] induced ACE2, as confirmed by densitometry normalized to vinculin controls (Fig. 4*B*). In contrast, hydroxychloroquine treatment was unable to consistently alter ACE2 or GLUL levels in a range of NSCLC cell lines (Fig. 4*C*), indicating this treatment is unable to alter EMT.

Together, these data suggest a potential model in which SARS-CoV-2 infects rare, epithelial, ACE2- and TMPRSS2-positive cells in the aerodigestive and respiratory tracts that are metabolically primed for glutamine synthesis and rapid replication (Fig. 4*D*). Once a cell is infected with SARS-CoV-2, there is a shift to a more mesenchymal phenotype characterized by high ZEB1 and AXL, putatively lower levels of miR-200, and a decreased dependence on glutamine synthesis. Viral infection and the resultant mesenchymal shift and ZEB1 increase may have devastating implications on the risk and pathogenesis of ARDS in patients with COVID-19 (Fig. 4*D*).

Discussion

The ultimate public health impact of the SARS-CoV-2 pandemic has not yet been fully realized. Although increased molecular understanding of the virus-host interactions is sorely needed, the impact of the pandemic itself has created practical limitations on laboratory-based research owing to wide-ranging institutional restrictions. Despite these restrictions, an unprecedented collaborative research effort has ensued, with little regard for geographic and public-private boundaries that so often impose their own limitations. In the above-mentioned study, we present an effort that not only incorporates our own unique cancer data sets but also uses a plethora of publicly available data from basic scientists, clinicians, and bioinformaticians around the world, including both normal and malignant tissues. The linkage of regulation of *ACE2* expression and EMT, the latter an uncommon phenomenon in normal tissue but well defined in cancer cells, highlights the value of considering malignant tissue and models for the investigation of SARS-CoV-2. Although tumor tissues and models undoubtedly have unique genetic and epigenetic features not routinely observed in nonmalignant SARS-CoV-2–infected cells in patients, many regulatory pathways and cellular behaviors, including those involved in EMT, are conserved between normal and malignant settings. Malignant tissues, however, offer a marked advantage than normal tissues in that they have been extensively profiled genomically, transcriptomically, and proteomically, including in circumstances in which processes such as EMT have been manipulated. The extent of available malignant tissue and model data, thus, allowed us to develop and preliminarily pursue novel hypotheses related to SARS-CoV-2 in data sets that were largely published before the emergence of the virus itself—another vital advantage when investigating a novel pathogen.

In this study, we describe a novel model for the regulation of ACE2, which others have found is essential for the host cell entry of SARS-CoV-2.[6] In contrast to reports of patient susceptibility to SARS-CoV-2 owing to age, gender, smoking history, or thoracic malignancies,[4,5,90,91] we were unable to identify consistent differences in ACE2 expression on the basis of these variables. Our data suggest that *ACE2* expression is restricted in both normal and malignant aerodigestive and respiratory tissues almost exclusively to epithelial cells, including highly specialized POU2F3-positive tuft cells, and that this restriction reflects regulatory mechanisms shared with EMT. Although others have observed a putative relationship in other contexts between ACE2 and EMT, these observations were inconsistent, supporting roles for ACE2 as an inducer and an inhibitor of EMT.[50,51] In virtually all explored datasets, ranging from cancer cell lines to normal respiratory tissue, we observed a strong and consistent negative correlation between *ACE2* expression and EMT. This relationship is observed even on a cell-by-cell basis, as scRNAseq illustrates that virtually every cell with detectable *ACE2* expression is epithelial on the basis of our published EMT score.[76]

The negative correlation between EMT and *ACE2* was not limited to expression analyses, as metabolomic analysis revealed that *ACE2* expression is strongly correlated with high levels of glutamine and the expression of *GLUL*, the enzyme responsible for the conversion of glutamate to glutamine. High levels of glutamine are characteristic of epithelial differentiation, whereas a shift from glutamine to glutamate is associated with EMT. We propose that SARS-CoV-2 targets these *ACE2*-expressing, metabolically primed epithelial cells to exploit the abundant nucleotides for rapid replication and viral spread. The consequence of SARS-CoV-2 infection is induction of EMT and subsequent up-regulation of GLS, resulting in a depletion of glutamine after SARS-CoV-2 infection in patients.[56]

Our subsequent analyses reveal that, beyond mere correlations, various strategies to manipulate EMT result in predictable alterations in the expression of *ACE2*. For example, treatment of cells with TGFβ or overexpression of ZEB1 induces EMT and decreased expression of *ACE2*. Similarly, in *EGFR*-mutant LUAD, in which there is

relatively higher *ACE2* expression, prolonged treatment with an *EGFR*-targeting TKI may result in multiple mechanisms of therapeutic resistance, of which EMT is a common one. Our results reveal that *ACE2* is down-regulated when EMT is the underlying resistance mechanism, but not when resistance emerges owing to development of secondary resistance mutations in *EGFR*. Coincident with the loss of *ACE2* expression is the down-regulation of *GLUL* to promote glutamate and enable production of tricarboxylic acid intermediates and energy.

EMT is a complex process regulated by an intricate molecular network, and we hoped to discern whether any of the specific pathway(s) that regulate EMT also mediate *ACE2* expression. An investigation into one of the transcriptional mechanisms underlying EMT and its association with *ACE2* revealed consistent positive correlations across tissue and sample types with the miR-200 family of miRNAs. The miR-200 family has a well-established role as an inhibitor of EMT by means of the down-regulation of the transcriptional repressor ZEB1. Predictably, a strong negative correlation was observed between *ACE2* and *ZEB1*. The repression of ACE2 by ZEB1 is mediated by means of two repressor binding sites for within the *ACE2* promoter, and forced overexpression of *ZEB1* results in a more than twofold decrease in *ACE2* expression, but not *GLUL*. ZEB1 regulation occurs by means of SNAI1 or TWIST1, whereas SNAI1 induces nuclear translocation of ETS1, which is required for ZEB1 expression.[92] It is likely that EMT induction of these genes by SARS-CoV-2 results in increased ZEB1. Finally, we observed that SARS-CoV-2–infected lung cancer cell lines, bronchial organoids, and patient nasopharyngeal swabs had substantial shifts toward several EMT-like features, including up-regulation of *ZEB1* and down-regulation of *EPCAM*.

Together, our data, in the context of the ever-growing literature on SARS-CoV-2, suggest that *ACE2* expression is necessary for initial viral entry and, therefore, is relatively high in those cells infected by the virus. These cells are epithelial and, in our data sets, unexpectedly rare, considering the devastating impact of this infection. After viral entry, however, SARS-CoV-2 infection induces molecular changes within the cells that are reminiscent of EMT—especially the increased expression of *ZEB1*. These SARS-CoV-2–induced changes, compounded by the down-regulation of genes, including tight junction components, which play a critical role in restricting epithelial and endothelial permeability, exposes respiratory cells to increased risk of edema and ARDS. Interestingly, previous reports with SARS-CoV(-1) reveal that lung cells, including alveolar-epithelial cells, express higher levels of TGFβ, a key regulator of EMT.[93] It is not surprising that a similar mechanism would occur with a similar coronavirus, such as SARS-CoV-2.

Although these data reveal an intriguing mechanism for the molecular virus-host interaction, it is critical to consider how these observations may be harnessed to develop strategies to improve patient outcomes. This, as always, is complex. Would a therapeutic effort focused on prevention of the initial infection by decreasing ACE2 levels, for example with an inhibitor of the miR-200 family, have unforeseen consequences, such as increased risk of ARDS? Similarly, would therapeutic efforts postinfection aimed at preventing SARS-CoV-2–induced ACE2 down-regulation, for example with a miR-200 mimetic, serve to place adjacent, newly ACE2-positive cells at risk for infection? Several large-cohort observational studies on ACE inhibitors and angiotensin II receptor blockers, which up-regulate ACE2 expression, did not reveal association with either SARS-Cov-2 infection or risk of severe COVID-19.[94] Interestingly, a human recombinant soluble ACE2, which has already been tested in phase 1 and phase 2 clinical trials for ARDS, revealed inhibition of SARS-CoV-2 infection in human capillary organoids and human kidney organoids.[95]

On the basis of the findings in our study, an attractive alternative therapeutic strategy would be to reverse EMT with an AXL inhibitor. AXL is overexpressed in several solid and hematologic malignancies, including NSCLC, acute myeloid leukemia, breast, and prostate cancer, among others. In the context of malignancy, AXL overexpression can drive EMT, tumor angiogenesis, and decreased antitumor immune response.[82] Furthermore, AXL inhibitor, gilteritinib, was identified to have antiviral activity against SARS-CoV-2.[96] Bemcentinib, a highly selective and potent inhibitor of AXL, is currently being tested in phase 2 trials in various malignancies, including NSCLC, acute myeloid leukemia, and breast cancer. In preclinical models, bemcentinib has already revealed potent antiviral activity in Ebola and Zika viruses.[38,97] Recent data suggest that bemcentinib inhibits SARS-CoV-2 viral entry into cells and prevents inhibition of type I interferon, which is the host cells' innate antiviral immune response. In contrast to AXL inhibition, hydroxychloroquine, an alternative treatment for patients with COVID-19, does not reveal any ability to reverse EMT. Accordingly, a phase II clinical trial (BGBC020) recently completed accrual of 115 patients, evaluating the efficacy and safety of bemcentinib for the treatment of hospitalized patients with COVID-19 alone or in combination with standard of care.[98] This trial reported a numerically lower number of deaths in the bemcentinib arm (one death in 28 patients) compared with the standard of care (five deaths in 32 patients), supporting our hypothesis that reversal of EMT in combination with antiviral activity warrants further investigation as a treatment for patients with clinically

significant SARS-CoV-2 infection.[99] Separately, a recent report independently identified both bemcentinib (AXL inhibitor) and dacomitinib (EGFR inhibitor) as possessing SARS-CoV-2 antiviral properties from 3000 drugs screened.[100] These data support our findings that EMT reversal by bemcentinib may augment the antiviral activity of AXL inhibitors against SARS-CoV-2, resulting in additional clinical benefit for patients with COVID-19.

CRediT Authorship Contribution Statement

C. Allison Stewart, Carl M. Gay, Lauren Averett Byers: Conceived the project, Analyzed and interpreted the data, Wrote the manuscript.

Kavya Ramkumar, Kasey R. Cargill: Performed the experiments, Interpreted the results.

Robert J. Cardnell, Monique B. Nilsson, Elizabeth M. Park, Carminia Maria Della Corte, Kiran Kundu: Interpreted the results.

Simon Heeke, Samrat T. Kundu, Lixia Diao, Qi Wang, Li Shen, Yuanxin Xi, Jing Wang: Contributed to the analysis and interpretation of data.

Curtis R. Pickering, Faye M. Johnson, Jianjun Zhang, Humam Kadara, John D. Minna, Don L. Gibbons, and John V. Heymach: Contributed to the acquisition of data, administrative, and/or material support.

C. Allison Stewart, Carl M. Gay, Kavya Ramkumar, Kasey R. Cargill, Robert J. Cardnell, Monique B. Nilsson, Simon Heeke, Elizabeth M. Park, Samrat T. Kundu, Lixia Diao, Qi Wang, Li Shen, Yuanxin Xi, Bingnan Zhang, Carminia Maria Della Corte, Youhong Fan, Kiran Kundu, Boning Gao, Kimberley Avila, Curtis R. Pickering, Faye M. Johnson, Jianjun Zhang, Humam Kadara, John D. Minna, Don L. Gibbons, Jing Wang, John V. Heymach, Lauren Averett Byers: Contributed to the writing, review, and/or revision of the manuscript.

Acknowledgments

We wish to acknowledge the patients affected by the coronavirus disease 2019 pandemic, along with their loved ones, the first responders, health care staff, and essential workers who worked tirelessly and selflessly during this devastating period. We thank C.E.S. for graphical elements and David M. Aten for assistance with medical illustrations. We thank P.M.G., M.P.B., W.A.B., G.D.S., P.W.S., R.A.S., R.R.S., R.A.D., B.A.D., V.J.M.C., S.C., S.C., J.P., S.I.1., S.I.2., and C.J.C. for intellectual support provided during quarantine. The work was supported by the National Institutes of Health (NIH)/National Cancer of Institute (NCI) R50-CA243698 (Dr. Stewart), NIH/NCI R01-CA207295 (Dr. Byers), NIH/NCI U01-CA213273 (Drs. Byers, Heymach), CCSG P30-CA01667 (Dr. Byers), University of Texas SPORE in Lung Cancer P5-CA070907 (Drs. Byers, Gibbons, Heymach, Gay, Wang, Ramkumar, Cargill), NIH/NCI R37CA214609 (Dr. Gibbons), the Department of Defense (LC170171; Byers), Khalifa Bin Zayed Al Nahyan Foundation (Dr. Gay), CPRIT Research Training Program RP170067 (Dr. Park), The International Association for the Study of Lung Cancer (Dr. Cargill), The University of Texas MD Anderson Cancer Center-Oropharynx Cancer Program generously supported by Mr. and Mrs. Charles W. Stiefel (Dr. Johnson), through generous philanthropic contributions to The University of Texas MD Anderson Lung Cancer Moon Shot Program, The Jane Ford Petrin Fund, The Andrew Sabin Family Fellowship, and The Rexanna Foundation for Fighting Lung Cancer.

Supplementary Data

Note: To access the supplementary material accompanying this article, visit the online version of the *Journal of Thoracic Oncology* at www.jto.org and at https://doi.org/10.1016/j.jtho.2021.07.002.

References

1. Wang C, Horby PW, Hayden FG, Gao GF. A novel coronavirus outbreak of global health concern. *Lancet*. 2020;395:470–473.
2. Zhu N, Zhang D, Wang W, et al. A novel coronavirus from patients with pneumonia in China, 2019. *N Engl J Med*. 2020;382:727–733.
3. Zhou P, Yang XL, Wang XG, et al. A pneumonia outbreak associated with a new coronavirus of probable bat origin. *Nature*. 2020;579:270–273.
4. Dai M, Liu D, Liu M, et al. Patients with cancer appear more vulnerable to SARS-COV-2: a multicenter study during the COVID-19 outbreak. *Cancer Discov*. 2020;10:783–791.
5. Yu J, Ouyang W, Chua MLK, Xie C. SARS-CoV-2 transmission in patients with cancer at a tertiary care hospital in Wuhan, China. *JAMA Oncol*. 2020;6:1108–1110.
6. Hoffmann M, Kleine-Weber H, Schroeder S, et al. SARS-CoV-2 cell entry depends on ACE2 and TMPRSS2 and is blocked by a clinically proven protease inhibitor. *Cell*. 2020;181:271–280.e8.
7. Cao Y, Li L, Feng Z, et al. Comparative genetic analysis of the novel coronavirus (2019-nCoV/SARS-CoV-2) receptor ACE2 in different populations. *Cell Discov*. 2020;6:11.
8. Imai Y, Kuba K, Rao S, et al. Angiotensin-converting enzyme 2 protects from severe acute lung failure. *Nature*. 2005;436:112–116.
9. Yang X, Yu Y, Xu J, et al. Clinical course and outcomes of critically ill patients with SARS-CoV-2 pneumonia in Wuhan, China: a single-centered, retrospective, observational study. *Lancet Respir Med*. 2020;8:475–481.
10. Kuba K, Imai Y, Rao S, et al. A crucial role of angiotensin converting enzyme 2 (ACE2) in SARS coronavirus-induced lung injury. *Nat Med*. 2005;11:875–879.

11. Cancer Genome Atlas Research Network. Comprehensive molecular profiling of lung adenocarcinoma. *Nature*. 2014;511:543–550.
12. Cancer Genome Atlas Research Network. Comprehensive genomic characterization of head and neck squamous cell carcinomas. *Nature*. 2015;517:576–582.
13. Tang H, Xiao G, Behrens C, et al. A 12-gene set predicts survival benefits from adjuvant chemotherapy in non-small cell lung cancer patients. *Clin Cancer Res*. 2013;19:1577–1586.
14. Kim ES, Herbst RS, Wistuba II, et al. The BATTLE trial: personalizing therapy for lung cancer. *Cancer Discov*. 2011;1:44–53.
15. Papadimitrakopoulou V, Lee JJ, Wistuba II, et al. The BATTLE-2 study: a biomarker-integrated targeted therapy study in previously treated patients with advanced non-small-cell lung cancer. *J Clin Oncol*. 2016;34:3638–3647.
16. Barretina J, Caponigro G, Stransky N, et al. Addendum: the Cancer Cell Line Encyclopedia enables predictive modelling of anticancer drug sensitivity. *Nature*. 2019;565:E5–E6.
17. Zhou BB, Peyton M, He B, et al. Targeting ADAM-mediated ligand cleavage to inhibit HER3 and EGFR pathways in non-small cell lung cancer. *Cancer Cell*. 2006;10:39–50.
18. Lockwood WW, Chari R, Coe BP, et al. DNA amplification is a ubiquitous mechanism of oncogene activation in lung and other cancers. *Oncogene*. 2008;27:4615–4624.
19. Kalu NN, Mazumdar T, Peng S, et al. Comprehensive pharmacogenomic profiling of human papillomavirus-positive and -negative squamous cell carcinoma identifies sensitivity to aurora kinase inhibition in KMT2D mutants. *Cancer Lett*. 2018;431:64–72.
20. Sun Y, Daemen A, Hatzivassiliou G, et al. Metabolic and transcriptional profiling reveals pyruvate dehydrogenase kinase 4 as a mediator of epithelial-mesenchymal transition and drug resistance in tumor cells. *Cancer Metab*. 2014;2:20.
21. Kundu ST, Byers LA, Peng DH, et al. The miR-200 family and the miR-183~96~182 cluster target Foxf2 to inhibit invasion and metastasis in lung cancers. *Oncogene*. 2016;35:173–186.
22. Nilsson MB Sun H, Robichaux J, et al. The YAP/FOXM1 axis regulates EMT-associated EGFR inhibitor resistance and increased expression of spindle assembly checkpoint components. *Sci Transl Med*. 2020;12:eaaz4589.
23. Raoof S, Mulford IJ, Frisco-Cabanos H, et al. Targeting FGFR overcomes EMT-mediated resistance in EGFR mutant non-small cell lung cancer. *Oncogene*. 2019;38:6399–6413.
24. Hata AN, Niederst MJ, Archibald HL, et al. Tumor cells can follow distinct evolutionary paths to become resistant to epidermal growth factor receptor inhibition. *Nat Med*. 2016;22:262–269.
25. Blanco-Melo D, Nilsson-Payant BE, Liu WC, et al. Imbalanced host response to SARS-CoV-2 drives development of COVID-19. *Cell*. 2020;181:1036–1045.e9.
26. Gibbons DL, Lin W, Creighton CJ, et al. Contextual extracellular cues promote tumor cell EMT and metastasis by regulating miR-200 family expression. *Genes Dev*. 2009;23:2140–2151.
27. Suzuki T, Itoh Y, Sakai Y, et al. Generation of human bronchial organoids for SARS-CoV-2 research. *bioRxiv*. https://www.biorxiv.org/content/10.1101/2020.05.25.115600v2.full.pdf. Accessed June 20, 2020.
28. Lieberman NAP, Peddu V, Xie H, et al. In vivo antiviral host transcriptional response to SARS-CoV-2 by viral load, sex, and age. *PLoS Biol*. 2020;18:e3000849.
29. Duclos GE, Teixeira VH, Autissier P, et al. Characterizing smoking-induced transcriptional heterogeneity in the human bronchial epithelium at single-cell resolution. *Sci Adv*. 2019;5:eaaw3413.
30. Puram SV, Tirosh I, Parikh AS, et al. Single-cell transcriptomic analysis of primary and metastatic tumor ecosystems in head and neck. *Cancer Cell*. 2017;171:1611–1624.e24.
31. Reyfman PA, Walter JM, Joshi N, et al. Single-cell transcriptomic analysis of human lung provides insights into the pathobiology of pulmonary fibrosis. *Am J Respir Crit Care Med*. 2019;199:1517–1536.
32. Vieira Braga FA, Kar G, Berg M, et al. A cellular census of human lungs identifies novel cell states in health and in asthma. *Nat Med*. 2019;25:1153–1163.
33. Kurppa KJ, Liu Y, To C, et al. Treatment-induced tumor dormancy through YAP-mediated transcriptional reprogramming of the apoptotic pathway. *Cancer Cell*. 2020;37:104–122:e12.
34. Gertz J, Savic D, Varley KE, et al. Distinct properties of cell-type-specific and shared transcription factor binding sites. *Mol Cell*. 2013;52:25–36.
35. Matsuyama S, Nao N, Shirato K, et al. Enhanced isolation of SARS-CoV-2 by TMPRSS2-expressing cells. *Proc Natl Acad Sci U S A*. 2020;117:7001–7003.
36. Ziegler CGK, Allon SJ, Nyquist SK, et al. SARS-CoV-2 receptor ACE2 is an interferon-stimulated gene in human airway epithelial cells and is detected in specific cell subsets across tissues. *Cell*. 2020;181:1016–1035.e1019.
37. Brindley MA, Hunt CL, Kondratowicz AS, et al. Tyrosine kinase receptor Axl enhances entry of Zaire ebolavirus without direct interactions with the viral glycoprotein. *Virology*. 2011;415:83–94.
38. Meertens L, Labeau A, Dejarnac O, et al. Axl mediates Zika virus entry in human glial cells and modulates innate immune responses. *Cell Rep*. 2017;18:324–333.
39. Chen J, Yang YF, Yang Y, et al. AXL promotes Zika virus infection in astrocytes by antagonizing type I interferon signalling. *Nat Microbiol*. 2018;3:302–309.
40. Brown J. University of Iowa virology research helps facilitate new clinical trial for COVID-19. University of Iowa Hospitals & Clinics. https://uihc.org/news/university-iowa-virology-research-helps-facilitate-new-clinical-trial-covid-19. Accessed June 26, 2020.
41. BerGenBio. BERGENBIO'S bemcentinib selected to be fast-tracked as potential treatment for COVID-19 through new national UK government clinical trial INITIATIVE. https://www.bergenbio.com/bergenbios-bemcentinib-selected-to-be-fast-tracked-as-potential-

treatment-for-covid-19-through-new-national-uk-government-clinical-trial-initiative/; 2020.
42. Spinato G, Fabbris C, Polesel J, et al. Alterations in smell or taste in mildly symptomatic outpatients with SARS-CoV-2 infection. *JAMA*. 2020;323:2089–2090.
43. Xydakis MS, Dehgani-Mobaraki P, Holbrook EH, et al. Smell and taste dysfunction in patients with COVID-19. *Lancet Infect Dis*. 2020;20:1015–1016.
44. Howitt MR, Lavoie S, Michaud M, et al. Tuft cells, taste-chemosensory cells, orchestrate parasite type 2 immunity in the gut. *Science*. 2016;351:1329–1333.
45. O'Leary CE, Schneider C, Locksley RM. Tuft cells-systemically dispersed sensory epithelia integrating immune and neural circuitry. *Annu Rev Immunol*. 2019;37:47–72.
46. Matsumoto I, Ohmoto M, Narukawa M, Yoshihara Y, Abe K. Skn-1a (Pou2f3) specifies taste receptor cell lineage. *Nat Neurosci*. 2011;14:685–687.
47. Ohmoto M, Yamaguchi T, Yamashita J, Bachmanov AA, Hirota J, Matsumoto I. Pou2f3/Skn-1a is necessary for the generation or differentiation of solitary chemosensory cells in the anterior nasal cavity. *Biosci Biotechnol Biochem*. 2013;77:2154–2156.
48. Yamashita J, Ohmoto M, Yamaguchi T, Matsumoto I, Hirota J. Skn-1a/Pou2f3 functions as a master regulator to generate Trpm5-expressing chemosensory cells in mice. *PLoS One*. 2017;12:e0189340.
49. Huang YH, Klingbeil O, He XY, et al. POU2F3 is a master regulator of a tuft cell-like variant of small cell lung cancer. *Genes Dev*. 2018;32:915–928.
50. Burns WC, Velkoska E, Dean R, Burrell LM, Thomas MC. Angiotensin II mediates epithelial-to-mesenchymal transformation in tubular cells by ANG 1–7/MAS-1-dependent pathways. *Am J Physiol Renal Physiol*. 2010;299:F585–F593.
51. Qian YR, Guo Y, Wan HY, et al. Angiotensin-converting enzyme 2 attenuates the metastasis of non-small cell lung cancer through inhibition of epithelial-mesenchymal transition. *Oncol Rep*. 2013;29:2408–2414.
52. Dongre A, Weinberg RA. New insights into the mechanisms of epithelial-mesenchymal transition and implications for cancer. *Nat Rev Mol Cell Biol*. 2019;20:69–84.
53. Park SM, Gaur AB, Lengyel E, Peter ME. The miR-200 family determines the epithelial phenotype of cancer cells by targeting the E-cadherin repressors ZEB1 and ZEB2. *Genes Dev*. 2008;22:894–907.
54. Title AC, Hong SJ, Pires ND, et al. Genetic dissection of the miR-200-Zeb1 axis reveals its importance in tumor differentiation and invasion. *Nat Commun*. 2018;9:4671.
55. Ramirez- Peña E, Arnold J, Shivakumar V, et al. The epithelial to mesenchymal transition promotes glutamine independence by suppressing *GLS2* expression. *Cancers (Basel)*. 2019;11:1610.
56. Shen B, Yi X, Sun Y, et al. Proteomic and metabolomic characterization of COVID-19 patient sera. *Cell*. 2020;182:59–72.e15.
57. Cheng ML, Chien KY, Lai CH, Li GJ, Lin JF, Ho HY. Metabolic reprogramming of host cells in response to enteroviral infection. *Cells*. 2020;9:473.
58. Fu X, Hu X, Li N, et al. Glutamine and glutaminolysis are required for efficient replication of infectious spleen and kidney necrosis virus in Chinese perch brain cells. *Oncotarget*. 2017;8:2400–2412.
59. Chambers JW, Maguire TG, Alwine JC. Glutamine metabolism is essential for human cytomegalovirus infection. *J Virol*. 2010;84:1867–1873.
60. Fontaine KA, Camarda R, Lagunoff M. Vaccinia virus requires glutamine but not glucose for efficient replication. *J Virol*. 2014;88:4366–4374.
61. Kim KK, Kugler MC, Wolters PJ, et al. Alveolar epithelial cell mesenchymal transition develops in vivo during pulmonary fibrosis and is regulated by the extracellular matrix. *Proc Natl Acad Sci U S A*. 2006;103:13180–13185.
62. Gouda MM, Shaikh SB, Bhandary YP. Inflammatory and fibrinolytic system in acute respiratory distress syndrome. *Lung*. 2018;196:609–616.
63. Herrero R, Sanchez G, Lorente JA. New insights into the mechanisms of pulmonary edema in acute lung injury. *Ann Transl Med*. 2018;6:32.
64. Ikenouchi J, Matsuda M, Furuse M, Tsukita S. Regulation of tight junctions during the epithelium-mesenchyme transition: direct repression of the gene expression of claudins/occludin by Snail. *J Cell Sci*. 2003;116:1959–1967.
65. Cao Y, Liu Y, Ping F, Yi L, Zeng Z, Li Y. miR-200b/c attenuates lipopolysaccharide-induced early pulmonary fibrosis by targeting ZEB1/2 via p38 MAPK and TGF-β/smad3 signaling pathways. *Lab Invest*. 2018;98:339–359.
66. Gay CM, Stewart CA, Park EM, et al. Patterns of transcription factor programs and immune pathway activation define four major subtypes of SCLC with distinct therapeutic vulnerabilities. *Cancer Cell*. 2021;39:346–360.e7.
67. Byers LA, Wang J, Nilsson MB, et al. Proteomic profiling identifies dysregulated pathways in small cell lung cancer and novel therapeutic targets including PARP1. *Cancer Discov*. 2012;2:798–811.
68. Chen L, Gibbons DL, Goswami S, et al. Metastasis is regulated via microRNA-200/ZEB1 axis control of tumour cell PD-L1 expression and intratumoral immunosuppression. *Nat Commun*. 2014;5:5241.
69. Li H, Ning S, Ghandi M, et al. The landscape of cancer cell line metabolism. *Nat Med*. 2019;25:850–860.
70. Fornes O, Castro-Mondragon JA, Khan A, et al. JASPAR 2020: update of the open-access database of transcription factor binding profiles. *Nucleic Acids Res*. 2020;48:D87–D92.
71. Jamieson AR, Giger ML, Drukker K, Li H, Yuan Y, Bhooshan N. Exploring nonlinear feature space dimension reduction and data representation in breast Cadx with Laplacian eigenmaps and t-SNE. *Med Phys*. 2010;37:339–351.
72. Byers LA, Diao L, Wang J, et al. An epithelial-mesenchymal transition gene signature predicts resistance to EGFR and PI3K inhibitors and identifies Axl as a

therapeutic target for overcoming EGFR inhibitor resistance. *Clin Cancer Res*. 2013;19:279–290.
73. Stewart CA, Gay CM, Xi Y, et al. Single-cell analyses reveal increased intratumoral heterogeneity after the onset of therapy resistance in small-cell lung cancer. *Nat Cancer*. 2020;1:423–436.
74. Kalu NN, Mazumdar T, Peng S, et al. Genomic characterization of human papillomavirus-positive and -negative human squamous cell cancer cell lines. *Oncotarget*. 2017;8:86369–86383.
75. Barretina J, Caponigro G, Stransky N, et al. The Cancer Cell Line Encyclopedia enables predictive modelling of anticancer drug sensitivity. *Nature*. 2012;483:603–607.
76. Mak MP, Tong P, Diao L, et al. A patient-derived, pan-cancer EMT signature identifies global molecular alterations and immune target enrichment following epithelial-to-mesenchymal transition. *Clin Cancer Res*. 2016;22:609–620.
77. Hmeljak J, Sanchez-Vega F, Hoadley KA, et al. Integrative molecular characterization of malignant pleural mesothelioma. *Cancer Discov*. 2018;8:1548–1565.
78. Alqahtani JS, Oyelade T, Aldhahir AM, et al. Prevalence, severity and mortality associated with COPD and smoking in patients with COVID-19: a rapid systematic review and meta-analysis. *PLoS One*. 2020;15:e0233147.
79. Di Stadio A, Ricci G, Greco A, de Vincentiis M, Ralli M. Mortality rate and gender differences in COVID-19 patients dying in Italy: a comparison with other countries. *Eur Rev Med Pharmacol Sci*. 2020;24:4066–4067.
80. Onder G, Rezza G, Brusaferro S. Case-fatality rate and characteristics of patients dying in relation to COVID-19 in Italy. *JAMA*. 2020;323:1775–1776.
81. Yaegashi H, Takahashi T. [Medical changes in preformed host arteries involved in a tumor-a morphometric study of gastric, colonic, and pancreatic carcinomas in man]. *Gan No Rinsho*. 1988;34:1555–1560.
82. Gay CM, Balaji K, Byers LA. Giving AXL the axe: targeting AXL in human malignancy. *Br J Cancer*. 2017;116:415–423.
83. Overgaard CE, Mitchell LA, Koval M. Roles for claudins in alveolar epithelial barrier function. *Ann N Y Acad Sci*. 2012;1257:167–174.
84. Allison Stewart C, Tong P, Cardnell RJ, et al. Dynamic variations in epithelial-to-mesenchymal transition (EMT), ATM, and SLFN11 govern response to PARP inhibitors and cisplatin in small cell lung cancer. *Oncotarget*. 2017;8:28575–28587.
85. Peng DH, Kundu ST, Fradette JJ, et al. ZEB1 suppression sensitizes KRAS mutant cancers to MEK inhibition by an IL17RD-dependent mechanism. *Sci Transl Med*. 2019;11:eaaq1238.
86. Peng DH, Ungewiss C, Tong P, et al. ZEB1 induces LOXL2-mediated collagen stabilization and deposition in the extracellular matrix to drive lung cancer invasion and metastasis. *Oncogene*. 2017;36:1925–1938.
87. Le X, Puri S, Negrao MV, et al. Landscape of EGFR-dependent and -independent resistance mechanisms to osimertinib and continuation therapy beyond progression in EGFR-mutant NSCLC. *Clin Cancer Res*. 2018;24:6195–6203.
88. Ray P, Wangzhou A, Ghneim N, et al. A pharmacological interactome between COVID-19 patient samples and human sensory neurons reveals potential drivers of neurogenic pulmonary dysfunction. *Brain Behav Immun*. 2020;89:559–568.
89. Holland SJ, Pan A, Franci C, et al. R428, a selective small molecule inhibitor of Axl kinase, blocks tumor spread and prolongs survival in models of metastatic breast cancer. *Cancer Res*. 2010;70:1544–1554.
90. Azulay RD, Velloso MB, Suguimoto SY, Ishida CE, Pereira Júnior AC. Acute disseminated paracoccidioidomycosis. Septic shock. *Int J Dermatol*. 1988;27:510–511.
91. Cai H. Sex difference and smoking predisposition in patients with COVID-19. *Lancet Respir Med*. 2020;8:e20.
92. Dave N, Guaita-Esteruelas S, Gutarra S, et al. Functional cooperation between Snail1 and twist in the regulation of ZEB1 expression during epithelial to mesenchymal transition. *J Biol Chem*. 2011;286:12024–12032.
93. Zuo W, Zhao X, Chen YG. SARS coronavirus and lung fibrosis. In: Lal S, ed. *Molecular Biology of the SARS-Coronavirus*. Berlin, Germany: Springer; 2009:247–258.
94. Jarcho JA, Ingelfinger JR, Hamel MB, D'Agostino RB Sr, Harrington DP. Inhibitors of the renin-angiotensin-aldosterone system and COVID-19. *N Engl J Med*. 2020;382:2462–2464.
95. Monteil V, Kwon H, Prado P, et al. Inhibition of SARS-CoV-2 infections in engineered human tissues using clinical-grade soluble human ACE2. *Cell*. 2020;181:905–913.e7.
96. Bouhaddou M, Memon D, Meyer B, et al. The global phosphorylation landscape of SARS-CoV-2 infection. *Cell*. 2020;182:685–712.e619.
97. Dowall SD, Bewley K, Watson RJ, et al. Antiviral screening of multiple compounds against Ebola virus. *Viruses*. 2016;8:277.
98. BerGenBio ASA. BerGenBio Closes Recruitment Into Trial Assessing Bemcentinib in COVID-19 Patients. Cision PR Newswire. https://www.prnewswire.co.uk/news-releases/bergenbio-closes-recruitment-into-trial-assessing-bemcentinib-in-covid-19-patients-817885187.html. Accessed March 5, 2021.
99. BerGenBio ASA. BerGenBio announces update from investigational phase II trials assessing bemcentinib in hospitalised COVID-19 patients. Cision PR Newswire. https://www.prnewswire.com/news-releases/bergenbio-announces-update-from-investigational-phase-ii-trials-assessing-bemcentinib-in-hospitalised-covid-19-patients-301271176.html. Accessed April 20, 2021.
100. Dittmar M, Lee JS, Whig K, et al. Drug repurposing screens reveal cell-type-specific entry pathways and FDA-approved drugs active against SARS-Cov-2. *Cell Rep*. 2021;35:108959.